

Received November 21, 2020, accepted December 14, 2020, date of publication December 17, 2020, date of current version December 31, 2020.

Digital Object Identifier 10.1109/ACCESS.2020.3045487

# Artificial Intelligence Vision-Based Monitoring System for Ship Berthing

HANGUEN KIM<sup>1</sup>, (Member, IEEE), DONGHOON KIM<sup>1</sup>, (Member, IEEE),  
BYEOLTEO PARK<sup>1</sup>, (Member, IEEE), AND SEUNG-MOK LEE<sup>2</sup>, (Member, IEEE)

<sup>1</sup>Seadronix Corporation, Seoul 06235, South Korea

<sup>2</sup>Department of Automotive System Engineering, Keimyung University, Daegu 42601, South Korea

Corresponding author: Seung-Mok Lee (seungmok@kmu.ac.kr)

This work was supported by the Keimyung University Research Grant of 2017-2018 under Grant 20170551 and Grant 20180652.

**ABSTRACT** This paper proposes a novel artificial intelligence vision-based monitoring system (AVMS) for ship berthing. To dock a ship, it is necessary to accurately estimate the relative distance between the quay wall and the ship. However, maneuvering large ships near a port is a complicated and difficult procedure. Thus, tugboats push the ship and dock it at the berth under the supervision of a pilot, who receives distance information from a berthing aid system (BAS). The conventional BAS based on laser distance sensors, which is the most widely used approach, is high-priced and limited by the size of the ship. Additionally, if there is an obstacle between the ship and the berth, the distance cannot be measured, since it obscures the laser signal. To address this problem, we develop an AVMS sensor module composed of a low-priced camera, a differential global positioning system (DGPS) receiver, and an inertial measurement unit (IMU) with an algorithm to estimate the distance between ship and berth. To evaluate the performance of the proposed AVMS, field tests are performed at Ulsan port in Korea, and the results are compared with a conventional BAS. From the field test results, the AVMS provides highly accurate estimates and shows robust performance in poor weather conditions compared to the conventional BAS. The AVMS can measure the distance between ship and berth regardless of the size of the ship, since it has a wide field of view. In addition, it provides the pilot with real-time image information of the ship approaching the berth to obtain safe ship berthing.

**INDEX TERMS** Artificial intelligence, berthing aid system (BAS), deep learning, vision sensor, ship berthing.

## I. INTRODUCTION

Due to the rapid development of the port logistics industry, ships are becoming larger, and marine traffic congestion is increasing. Therefore, port operations focus on the rapid and safe berthing and unberthing of large container ships. However, berthing maneuvers are performed by tugboats, since maneuvering large ships near the port is a complicated and difficult procedure [1]. Many accidents occur when ships approach ports since neither the surrounding environment of the ship nor the port environment can be accurately identified by the pilot. Accidents in ports cause significant monetary damage, injury, and major risks in port operation.

The associate editor coordinating the review of this manuscript and approving it for publication was Zhenhua Guo<sup>1</sup>.

To address this problem, various sensor-based berthing aid systems (BASs) have been applied, e.g., laser distance sensors, lidar, radar, and cameras. An approach based on a pair of 1D laser distance sensor-based BAS is currently the most widely used approach in actual ports [2], [3]. However, it incurs high costs for installation, operation, and maintenance. In addition, because the laser distance sensors are fixed at specific locations in the port and cannot be moved, there is a limit to the sizes of ships that can be recognized. In [4], a 3D lidar-based monitoring system was proposed to overcome the limitations in regard to the accuracy of a 1D laser distance sensor-based BAS. However, the measurement data are noisy in poor weather conditions, including rain, haze, and snow, because of the scattering and diffuse reflection of laser light.

Radar-based BAS is robust against environmental changes [5]. However, when the ship approaches the berth, the radar signals can contain large errors caused by multiple and indirect echoes reflected from floating obstacles or berth facilities. Therefore, radar-based BAS can cause unreliable ship berthing [1].

Recently, a markerless distance measurement system for ship berthing has been proposed based on stereo cameras [6], [7]. Two stereo cameras are used to measure the distances to the bow and stern of the ship. However, the proposed system is a prototype, tested at a distance of up to only 25 m, and its performance degrades under illumination changes.

Electronic chart display and information systems (ECDISs) and automatic identification systems (AISs) are also used for ship berthing. Since these devices use location information measured based on the global positioning system (GPS) data of each ship, there are limitations of inaccuracies in GPS, insufficient update periods, and ships not registered with the AIS. Therefore, there is a very high demand for technology that can monitor the vicinity of a ship or a port through video for safe and rapid berthing and for low-cost systems to address the problems in existing systems.

The purpose of this paper is as follows. We propose a novel artificial intelligence vision-based monitoring system (AVMS) for ship berthing; this system is more economical and overcomes the disadvantages in the conventional laser distance sensor-based BAS. The proposed system provides precise and accurate measurements of the distances between port and ship regardless of the environmental and illumination conditions when the ship is berthing. In addition, although conventional approaches have limitations regarding the size of the ship that can be recognized, the proposed system has no limitations on the size of the ship. The proposed AVMS sensor module comprises a camera, a differential GPS (DGPS) receiver, and an inertial measurement unit (IMU). In addition, the AVMS can robustly recognize ships even in poor weather conditions, by applying the deep learning model in [8] to overcome the inherent limitations of the camera.

The remainder of this paper is organized as follows. In Section II, a conventional laser distance sensor-based BAS is briefly reviewed, and its limitations are discussed. Section III describes the proposed AVMS hardware and software systems. Section IV presents field test results based on various environmental conditions. Finally, a conclusion is presented in Section V.

## II. CONVENTIONAL APPROACH

### A. LASER DISTANCE SENSOR-BASED BERTHING AID SYSTEM (BAS)

Laser distance sensor-based BASs are the most widely used assistant systems for ship berthing [2]. The basic concept of the conventional laser distance sensor-based BASs is shown in Fig. 1. Two laser distance sensors are mounted at the

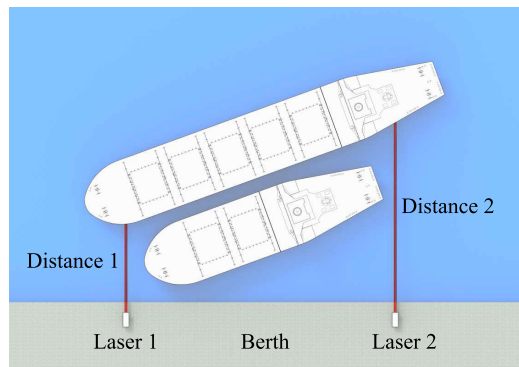


**FIGURE 1. Conventional berthing aid system (BAS) based on a pair of laser distance sensors. Conventional BAS systems have the following limitation: if the size of the ship is too small, the laser distance sensors may not be able to estimate the distance from the ship to the berth.**

berth. One sensor measures the distance from the berth to the ship's bow, and the other measures the distance from the berth to the ship's stern. The BAS provides the approaching distance information of the ship to the pilot and ground crews to prevent collisions due to excessive speed, and the BAS helps ships safely reach the berths. Under good weather conditions, the maximum measurable distance of a typical BAS is approximately 100-150 m.

### B. LIMITATIONS OF THE LASER DISTANCE SENSOR-BASED BAS

Laser distance sensor-based BAS systems have the following limitations. Because two laser distance sensors are fixed at specific locations in the berth, as shown in Fig. 1, the BAS system has a limit on the size of the ship that can be measured. If the size of the ship is too small or too large, the laser range sensors may not accurately point the bow and stern of the ship and consequently cannot estimate an accurate distance and speed.

Many obstacles can float near the berth, and the speed and distance information between such obstacles and the ship is also very important for safely docking the ship. However, the conventional laser distance sensor-based BAS cannot detect floating obstacles, such as other ships near the berth. The high sensor price and construction costs of the conventional BAS have also been emphasized as problems.

## III. ARTIFICIAL INTELLIGENCE VISION-BASED MONITORING SYSTEM (AVMS)

### A. SYSTEM SPECIFICATION AND OVERVIEW

To overcome the limitations of the conventional laser distance sensor-based BAS, we propose an AVMS for ship berthing. The purpose of the AVMS is to inform pilots and ground crews of navigation information generated by fusing the sensor data gathered from multiple AVMS sensor modules at the berth. Basically, the AVMS estimates the relative distance from the berth to the bow and stern of the ship. In addition, it recognizes obstacles and other ships nearby and estimates the relative positions to prevent collisions. If a collision is

detected, the AVMS warns the pilots and ground crew to prevent marine ship accidents.

The sensor module of the AVMS is composed of a wide-angle camera for image capture, a DGPS for precise positioning, an IMU for attitude measurement, an embedded computer for software implementation, and the local area network (LAN), as shown in Fig. 2. Each sensor module is enclosed in a waterproof case to prevent corrosion from seawater. The sensor modules are installed in a fixed structure near the berth and at a certain height from sea level. The postures of the sensor modules are designed to be manually or automatically adjusted. Table 1 shows the main specifications of the AVMS sensor module, e.g., the measuring item, field of view, sampling rate, operating illuminance, and international protection (IP) code. Since the maximum approach speed of the ship is less than 1 m/s during berthing, the sampling rate for distance estimation near the port generally requires 1 Hz. In addition, the AVMS can provide real-time video data to pilots and ground crews through a cloud server at a sampling rate of 10 Hz. The IP67 rating indicates that the system can provide complete protection against the ingress of dust and water.

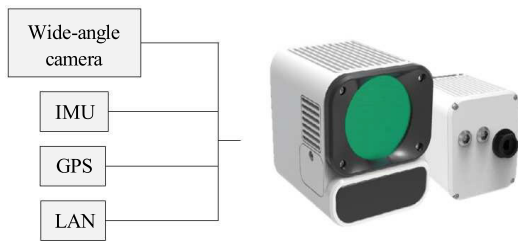


**FIGURE 2.** Components of the artificial intelligence vision-based monitoring system for the ship berthing (AVMS) sensor module. Each sensor module consists of a wide-angle camera, a DGPS, an IMU, an embedded computer, and the local area network (LAN).

**TABLE 1.** Main specifications.

Measuring item	Distances from ships to the berth
Field of view	150 m (longitudinal) × 300 m (lateral)
Sampling rate	1 Hz
Operating illuminance	100 Lux to 20,000 Lux
IP code	IP67

The AVMS hardware system consists of multiple AVMS sensor modules, a local server, and a cloud server, as shown in Fig. 3. To ensure a wide field of view, multiple AVMS sensor modules are installed in a berth to collect the sensor data. Each sensor module preprocesses image data by fusing the IMU and DGPS data in an embedded computer based on NVIDIA Jetson TX2 [9]. The preprocessed images are transferred to the local server via LAN. The local server stitches the images collected from multiple AVMS sensor modules to generate a wide-angle image to estimate the relative distances of the ship from the berth. The relative distance estimates and wide-angle images of the ships are transmitted in real time to a cloud server through a 4G or 5G cellular network.

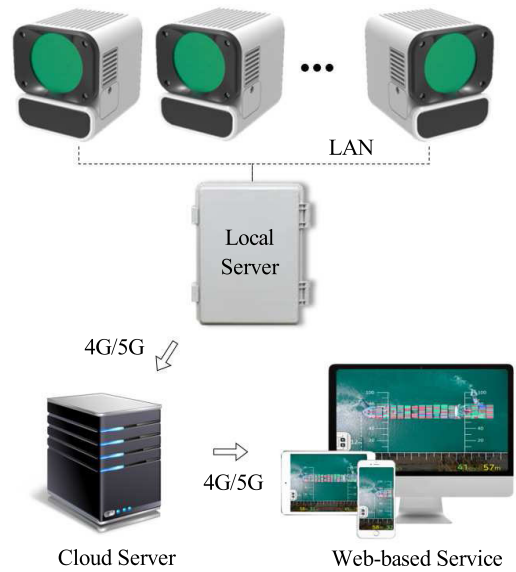


**FIGURE 3.** Overview of the AVMS hardware system consisting of multiple AVMS sensor modules, a local server, and a cloud server. The cloud server provides web-based services to the users.

The cloud server provides users with the location information of the ships and wide-angle images, which can be interpreted at a glance. Fig. 4 schematically shows the sensor data preprocessing performed on the embedded computer of each sensor module, and the relative distance estimation algorithm performed on the local server. Details of the preprocessing of the sensor data and relative distance estimation algorithm are described in Sections III-B and III-C, respectively.

## B. IMAGE PREPROCESSING

### 1) IMAGE ENHANCEMENT

In marine environments, large daily temperature ranges and evaporation of seawater from haze frequently occur, which make the image-based ship recognition difficult. Deep learning [10] and image processing [11], [12]-based image enhancement algorithms have been proposed for noise reduction in general environments. However, these image enhancement algorithms are not suitable for operation in an embedded computer, since they require large amounts of computation. Therefore, we apply the image enhancement algorithm proposed by K. He [12] to the AVMS by optimizing and simplifying it to be suitable for real time operation in the embedded computer to eliminate haze. Fig. 5 shows the results of the enhancement algorithm on a raw image with haze.

### 2) SHIP DETECTION AND SEGMENTATION

An object segmentation algorithm is used to detect the ship to be tracked and distinguish it from floating obstacles, other ships, and the surrounding environment based on the images collected by the AVMS. The AVMS uses a deep learning-based Skip-ENet [8] model to recognize objects in real time from images. The Skip-ENet model is designed to

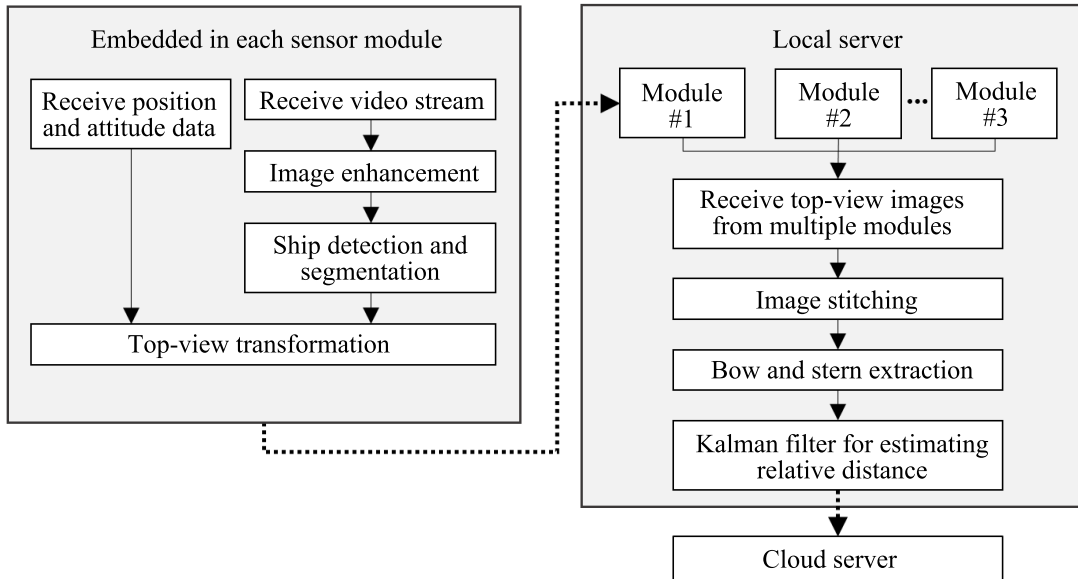


**FIGURE 4.** Overview of the AVMS software system. An embedded computer of each sensor module preprocesses the sensor data. A local server estimates the relative distances by stitching the images from multiple AVMS sensor modules.



**FIGURE 5.** Source image (left) and enhanced image (right).

recognize marine objects such as boats and buoys in various marine environments. Since it can extract marine objects in pixel units, it is suitable for estimating the shape information of objects. In [8], the Skip-ENet model shows the best segmentation performance in a marine environment compared to other deep learning models for segmentation. In addition, Skip-ENet can be implemented in the embedded computing unit of the AVMS and reduce the amount of computation by up to 1/100 compared to other deep learning models.

Fig. 6(a) is the raw image obtained from the AVMS camera, and Fig. 6(b) shows the segmentation result from the Skip-ENet [8] processing of the raw image. Objects on the sea surface, such as ships and floating obstacles, are marked in red, the sea surface is marked in blue, and other areas are marked in white. Among the object areas marked in red, noises such as those from sea clutter, small boats, floating objects, and coastal terrains are removed. From the results, the target ship can be selected, and the quay wall can be detected.

### 3) TOP-VIEW TRANSFORMATION AND IMAGE STITCHING

The AVMS collects images from each wide-angle camera and stitches them into a single image to recognize a berth area of approximately 300 m in lateral length so that the entire area

can be simultaneously observed. Each image is transformed into a top-view using an inverse perspective mapping (IPM) algorithm [13]–[17]. The IPM uses the position and attitude information of the camera to produce a top-view image to remove perspective effects.

The process of transformation into a top-view based on the DGPS and IMU sensors is as follows. Let  $[X_w, Y_w, Z_w]^T$  be the world coordinate system,  $[X_c, Y_c, Z_c]^T$  be the camera's coordinate system, and  $[U, V]^T$  be the image coordinate system, as shown in Fig. 7. The purpose of IPM is to transform a pixel point  $[u, v]^T$  on the image coordinate system to a 3D position  $[x, y, z]^T$  on the world coordinate system, and the relationship between the two coordinate systems can be expressed as [13], [17]:

$$\lambda \begin{bmatrix} u \\ v \\ 1 \end{bmatrix} = \mathbf{K} [\mathbf{R} | \mathbf{T}_c] \begin{bmatrix} x \\ y \\ z \\ 1 \end{bmatrix}, \quad (1)$$

where  $\lambda$  is the homogeneous scaling factor, and  $\mathbf{K}$  is a  $3 \times 3$  matrix that represents the intrinsic parameter of the camera represented as

$$\mathbf{K} = \begin{bmatrix} \alpha_x & \beta & u_0 \\ 0 & \alpha_y & v_0 \\ 0 & 0 & 1 \end{bmatrix}. \quad (2)$$

The parameters of  $\alpha_x$  and  $\alpha_y$  are the lens scaling factors,  $u_0$  and  $v_0$  the principal point, and  $\beta$  the skewness factor. The  $3 \times 3$  rotation transformation matrix  $\mathbf{R}$  rotates the camera's coordinate system to the world coordinate system in 3D that can be obtained by measurements of the IMU. The  $3 \times 1$  translation vector  $\mathbf{T}_c$  is the origin of the world coordinate system expressed in the camera coordinate system that can be

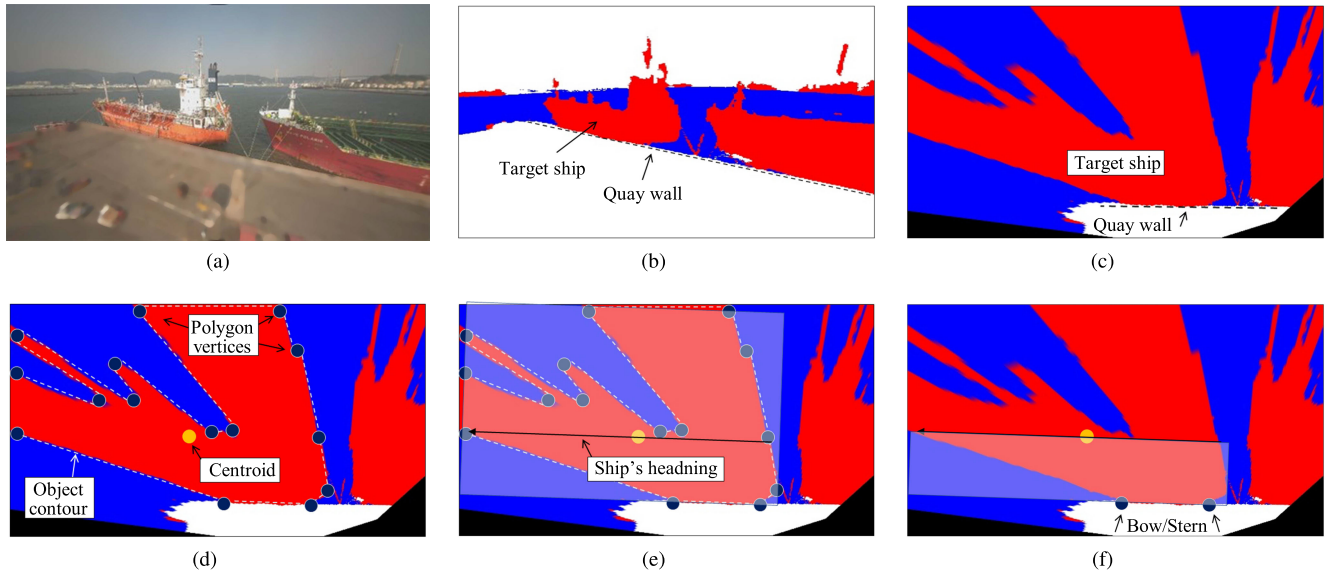


**FIGURE 6.** (a) Raw image as received from the AVMS camera. (b) Raw image as segmented by Skip-ENet [8]. Pixels representing the objects are in red, the sea surface is in blue, and other areas are in white. (c) The AVMS transforms the image into a top-view based on the sea level, which indicates that the direction of the quay wall of the berth is aligned with the horizontal direction in the image. (d) The contour of the ship is extracted, and its centroid is computed. Then, the contour is approximated into a polygon. (e) The white opaque box represents the smallest area that contains all polygon vertices, and the direction of the longest side of the rectangle can be considered the heading of the ship. (f) The rectangle that contains all polygon vertices can be reduced to include only the hull area. Among the vertices in the reduced rectangle, the two closest vertices to the quay wall are considered the bow and stern.

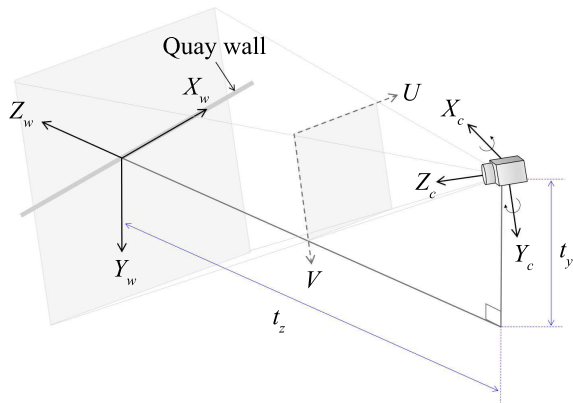


**FIGURE 7.** The relationship between the world coordinate system  $[X_w, Y_w, Z_w]^T$ , the camera's coordinate system  $[X_c, Y_c, Z_c]^T$ , and the image coordinate system  $[U, V]^T$ .

obtained by measurements of the DGPS. The AVMS sensor module is usually stationary, but it is possible to manually or automatically change the attitude of the camera when adjusting the field of view according to the size of the ship, i.e., if the position or attitude of the AVMS sensor module is changed, it is estimated through the IMU and DGPS. If the projection plane is the plane at sea level, the constraint of the plane is expressed as  $y = y_0$  and can be included in (1) as follows:

$$\lambda \begin{bmatrix} u \\ v \\ 1 \\ 0 \end{bmatrix} = \left[ \begin{array}{ccc|c} \mathbf{KR} & & & -\mathbf{KRT}_w \\ 0 & 1 & 0 & -y_0 \end{array} \right] \begin{bmatrix} x \\ y \\ z \\ 1 \end{bmatrix} = \mathbf{M} \begin{bmatrix} x \\ y \\ z \\ 1 \end{bmatrix}^T. \quad (3)$$

where  $\mathbf{T}_w = [t_x, t_y, t_z]^T$  is the translation vector between the two coordinate systems expressed in the world coordinate system, i.e., the relationship between  $\mathbf{T}_c$  and  $\mathbf{T}_w$  can be represented as  $\mathbf{T}_c = -\mathbf{RT}_w$ . Through the inverse transformation of (3), image pixels  $[u, v]^T$  can be mapped to  $[x, y, z]^T$  on the sea level with  $y = y_0$  as follows:

$$\begin{bmatrix} x & y & z & 1 \end{bmatrix}^T = \lambda \mathbf{M}^{-1} \begin{bmatrix} u & v & 1 & 0 \end{bmatrix}^T. \quad (4)$$

To obtain the solution of (4),  $\mathbf{M}$  should be always invertible. If the determinant of  $\mathbf{M}$  is nonzero, then  $\mathbf{M}$  is invertible. The determinant of  $\mathbf{M}$  can be computed as

$$\det \left( \left[ \begin{array}{ccc|c} \mathbf{KR} & & & -\mathbf{KRT}_w \\ 0 & 1 & 0 & -y_0 \end{array} \right] \right) = \det(\kappa) \det(\mathbf{KR}) = \kappa \det(\mathbf{KR}), \quad (5)$$

where

$$\begin{aligned} \kappa &= -y_0 - [0 \ 1 \ 0] (\mathbf{KR})^{-1} (-\mathbf{KRT}_w) \\ &= -y_0 + [0 \ 1 \ 0] \mathbf{T}_w \\ &= -y_0 + t_y. \end{aligned} \quad (6)$$

If  $t_y \neq y_0$ , then  $\kappa$  is nonzero. Also, since  $\det(\mathbf{K}) > 0$  and  $\det(\mathbf{R}) = 1$ , the condition that  $\det(\mathbf{KR}) \neq 0$  is always satisfied. From these results,  $\det(\mathbf{M})$  is nonzero while satisfying  $t_y \neq y_0$ . Thus, the solution of (4) can be obtained.

The AVMS transforms each image into a top-view based on a plane at sea level, so that the direction of the quay wall of the berth is aligned with the horizontal direction on the image. Fig. 6(c) is a top-view transformed image based on the result of Fig. 6(b). As shown in Fig. 6(c), the area corresponding to the upper part of the ship's deck is distorted. However,

since the IPM is performed based on sea level, the perspective effect on the quay wall of the berth and the intersection line between the hull and the sea surface can be eliminated. Even if the installation position or attitude of the camera is changed, the plane remains the same, which makes it easy to match the images. In addition, moving objects on the sea level can be estimated in the two-dimensional coordinate system.

The local server collects the top-view images from multiple AVMS sensor modules to obtain a wide field of view. When performing the top-view image transformation in the local server, a common world coordinate system is used for all AVMS sensor modules. Since all top-view images received from multiple AVMS sensor modules are based on the common world coordinate system, image stitching can be easily performed.

### C. RELATIVE DISTANCE ESTIMATION

#### 1) BOW AND STERN EXTRACTION

The process of extracting the bow and stern of the ship from the image and estimating the distance from the bow and stern to the quay wall of the berth is as follows. As shown in Fig. 6(d), we detect the object contour for the area that corresponds to the target ship object and find the centroid of the contour. Then, the object contour is approximated into a polygon. To compute the heading of the ship, we find the rectangle with the smallest area that contains all polygon vertices, as indicated by the white opaque box in Fig. 6(e). Among the four sides of the rectangle, the longest side that is closest to the quay wall is considered the line where the hull and sea level are in contact, and the direction parallel to this line is considered the heading of the ship. As shown in Fig. 6(f), the rectangle can be reduced to include only the hull area based on the heading and center point of the ship. Among the vertices of the polygon within the reduced rectangle, the two closest vertices to the quay wall are considered the bow and stern of the ship.

#### 2) KALMAN FILTER TO ESTIMATE THE RELATIVE DISTANCE

The distances from the bow and stern to the quay wall are estimated by a Kalman filter. We denote a state vector  $\mathbf{x}_k^{bow} = [d_k^{bow}, \dot{d}_k^{bow}]$ , where  $d_k^{bow}$  and  $\dot{d}_k^{bow}$  are the distances from the quay wall to the bow and approaching speed at time step  $k$ , respectively. The process model and measurement model are as follows:

$$\mathbf{x}_{k+1} = \mathbf{A}\mathbf{x}_k + \mathbf{w}_k, \quad (7)$$

$$\mathbf{z}_k = \mathbf{H}\mathbf{x}_k + \mathbf{v}_k, \quad (8)$$

$$\mathbf{A} = \begin{bmatrix} 1 & \Delta t \\ 0 & 1 \end{bmatrix}, \quad (9)$$

$$\mathbf{H} = \begin{bmatrix} 1 & 0 \end{bmatrix}, \quad (10)$$

where  $\mathbf{w}_k$  and  $\mathbf{v}_k$  are the normally distributed process noise and measurement noise, respectively. Since the approaching speed of the ship is generally very slow (e.g., several cm/s), the speed estimated in the previous time step is assumed to



FIGURE 8. Experimental setup with two AVMS sensor modules. The AVMS sensor modules are currently installed at Ulsan port in Korea and being pilot tested.

TABLE 2. Distance error.

Distance	Bow		Stern	
	Mean	Std	Mean	Std
80 m-60 m	3.8993	0.8214	1.2491	0.5786
60 m-40 m	0.7210	0.5732	1.5247	0.3800
40 m-20 m	1.5023	0.4976	0.2590	0.1952
< 20 m	N/A	N/A	0.1358	0.0869
Total	0.8115	0.6820	0.3712	0.5203

be identical. This Kalman filter is also applied to estimate the distance from the stern to the quay wall.

### IV. FIELD TEST VALIDATION

To evaluate the performance of the proposed AVMS, real-world field tests were performed based on a large ship at Ulsan port in Korea. Two sensor modules were installed, as shown in Fig. 8, to cover an area of 300 m (lateral)  $\times$  100 m (longitudinal) from the port: one observes the bow, and the other observes the stern. To compare the performances in various environments, the distances from the quay wall to the bow and stern of the ship were measured in real time in daytime, nighttime, and rainy environments. To compare the accuracy and precision of the distance measured from the AVMS, a 16-channel lidar was used to implement the conventional laser distance sensor-based BAS in Fig. 2. The measured distances to the bow and stern were compared for a large ship, which was approximately 150 m long. The lidar-based BAS measurement values in the daytime environment were considered reference values and compared with the AVMS results, since the BAS results provide stable measurements in an ideal environment such as daytime.

Fig. 9 shows the test results of the AVMS and lidar-based BAS operations during a normal clear day. The green line represents the bottom of the ship in contact with the sea surface as estimated by the AVMS; the black line represents the edge of the quay wall. The red points represent the point cloud as measured from the lidar, and the gray lines represent the distance to the bow and stern, as estimated by the lidar-based BAS. As seen in the results, when the ship is located 300 m away from the port, the BAS system cannot measure the distance, since the ship has not entered the field of view of the lidar-based BAS. However, the AVMS measures the

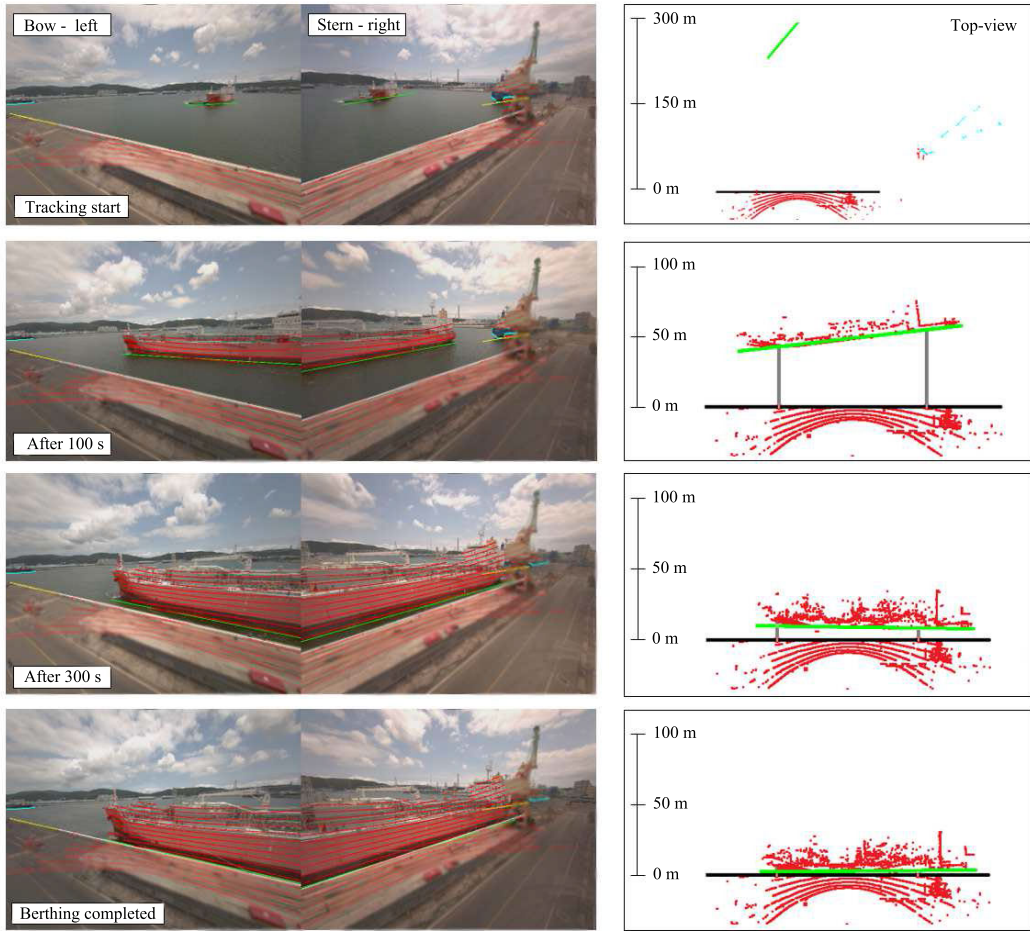


**FIGURE 9.** Field test result during the daytime on a clear day. The green line represents the bottom of the hull that is in contact with the sea surface, and the black line represents the edge of the quay wall. The red points represent the point cloud of the lidar, and the gray lines represent the distances to the bow and stern, which are estimated by the lidar-based BAS.

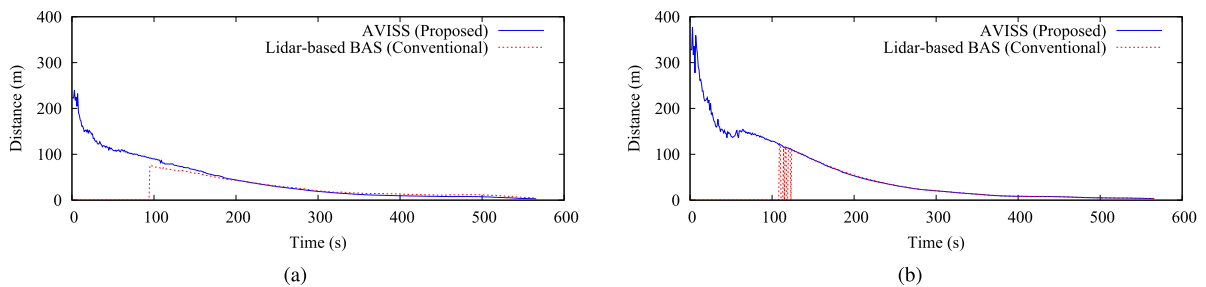


**FIGURE 10.** Comparison of the distances estimated by the field test during the daytime on a clear day. (a) From the quay wall to the bow; (b) from the quay wall to the stern.

position of the ship until the ship finally completes the berthing.

Fig. 10 shows the measured straight line distances from the quay wall to the bow and stern by the AVMS and lidar-based BAS when the ship approaches the berth, respectively. The results show that the lidar-based BAS starts measuring when the ship is within 100 m from the port. Table 2 shows the distance error for each section by dividing

the approach distance into sections of 20 m when the ship approaches the port. The accuracy and precision increase when the ship approaches the port. Since the bow of the ship is curved, the measurement of the BAS is inaccurate at distances below 20 m; thus, the BAS signal should not be used as a reference signal. These results show that the low-cost AVMS can be a suitable alternative to the existing high-cost BAS.

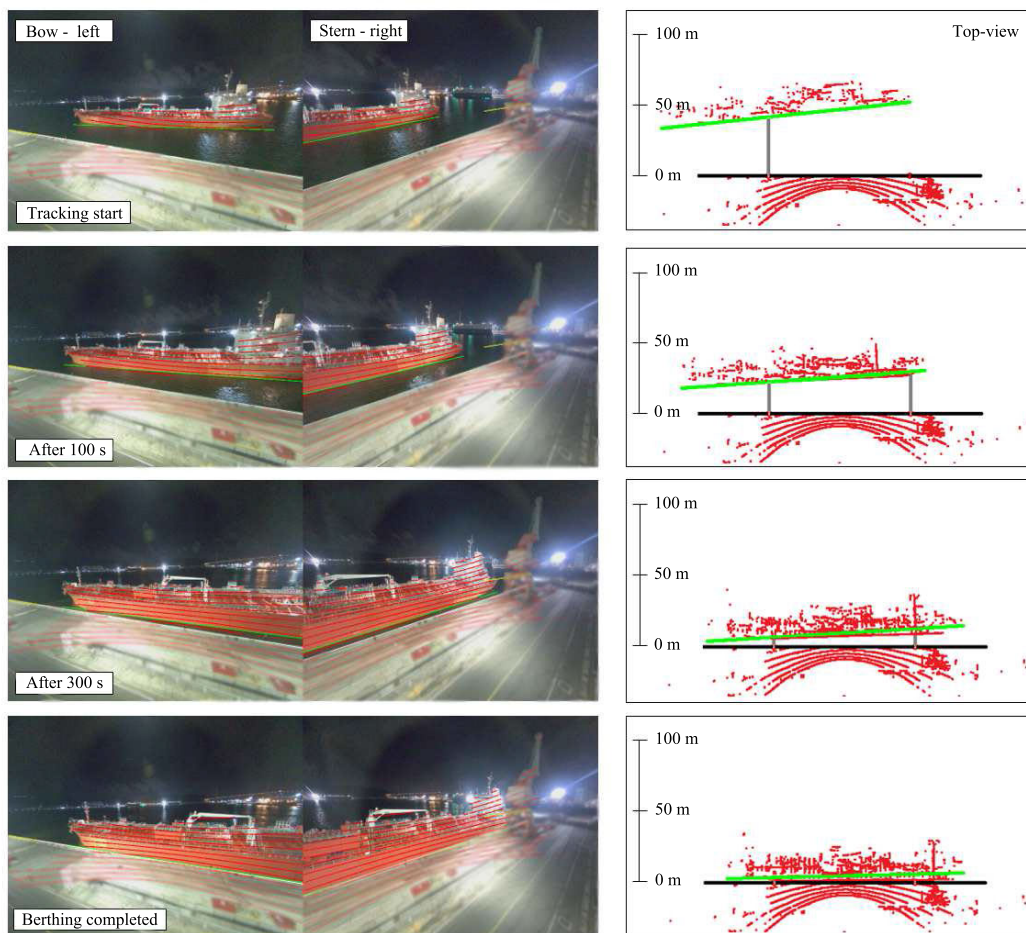


FIGURE 11. Field test result at night on a clear day.

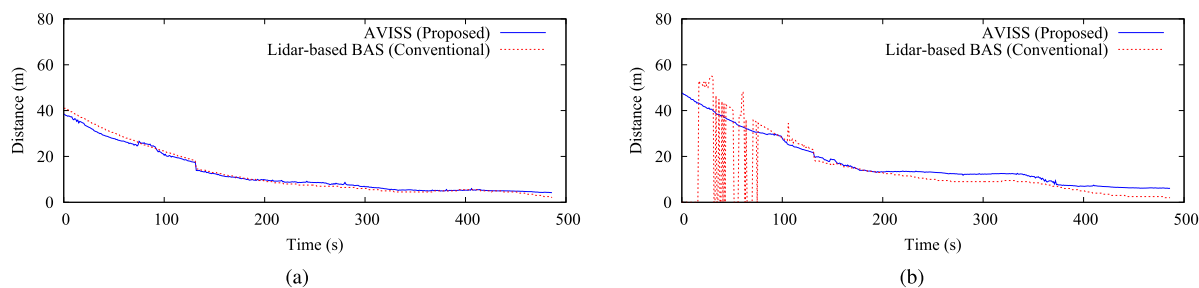


FIGURE 12. Comparison of the distances estimated by the field tests at night on a clear day. (a) From the quay wall to the bow; (b) from the quay wall to the stern.

In addition, to test the robustness of the AVMS with respect to environmental changes, additional experiments were conducted at night and on rainy days. Figs. 11 and 12 show the results of field tests at night on clear days. From the first top-view image in Fig. 11, the stern clearly cannot be measured, since the entire ship does not enter the field of view of the BAS, although the ship approaches at a distance of approximately 50 m from the berth. However, even at night, the AVMS recognizes the entire ship and the distance from the

berth to the ship. Figs. 13 and 14 show the field test results from a rainy night. In general, the BAS works well in all light conditions, but its performance degrades in snowy, foggy, and rainy environments, because of the irregular reflection of the laser light. Fig. 14 shows that the measurement by the BAS is not stable under rainy conditions. However, the AVMS maintains stable performance even in a rainy environment at night, and the measurements are continuously made without interruption.



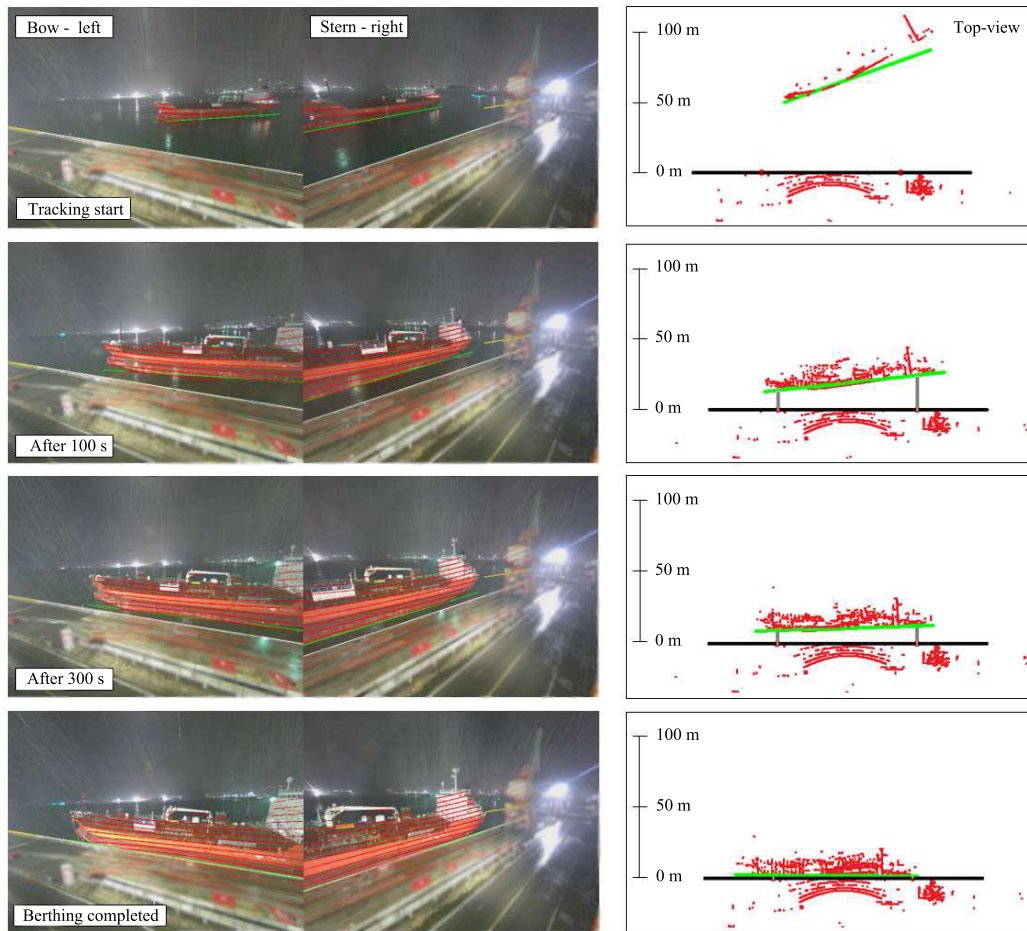


FIGURE 13. Field test result at night on a rainy day.

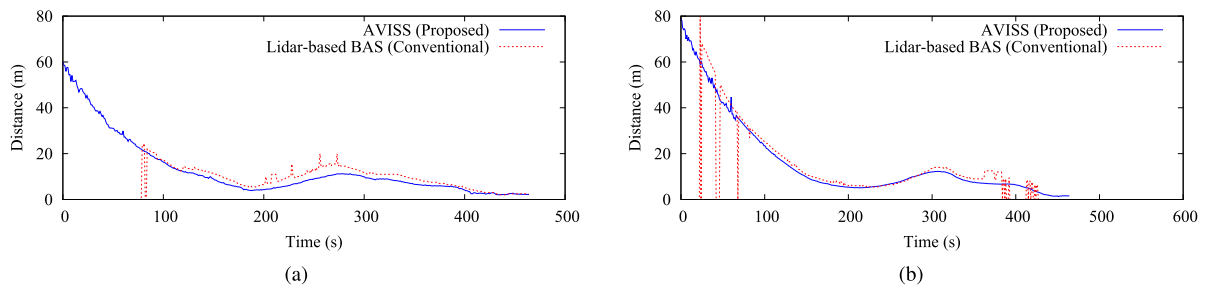


FIGURE 14. Comparison of the distances estimated by the field tests at night on a rainy day. (a) From the quay wall to the bow; (b) from the quay wall to the stern.

V. CONCLUSION

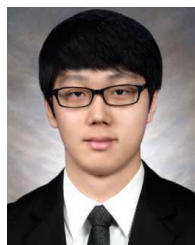
This paper proposed a novel AVMS, which is a monitoring system based on artificial intelligence vision for ship berthing. To provide an alternative to the high-cost laser distance sensor-based BAS, the AVMS sensor module consists of relatively low-cost sensors such as a camera, a DGPS receiver and an IMU. An image processing algorithm estimates the distance between the ship and the berth by fusing the sensor data obtained from multiple AVMS sensor modules. To evaluate the performance of the proposed AVMS,

field tests were conducted in various environments based on real ships at Ulsan port in Korea, and the results were compared with those from a lidar-based BAS system. The field test results show that the AVMS performed better than the conventional BAS, which can provide accurate distance measurements in an ideal environment. In addition, the AVMS showed more robust performance than an existing BAS system in bad weather conditions. The AVMS has a wide field of view and can measure the distance to the berth regardless of the size of the ship. In conclusion, AVMSs, which are

relatively inexpensive, can be a suitable alternative to the existing high-priced laser distance sensor-based BASs, and they can be applied in actual ports.

## REFERENCES

- [1] V.-S. Nguyen, V.-C. Do, and N.-K. Im, "Development of automatic ship berthing system using artificial neural network and distance measurement system," *Int. J. FUZZY Log. Intell. Syst.*, vol. 18, no. 1, pp. 41–49, Mar. 2018.
- [2] Y. Yu, B. Zhao, H. Zhu, and L. Yang, "Berthing support system using laser and marine hydrometeorological sensors," in *Proc. IEEE 3rd Inf. Technol. Mechatronics Eng. Conf. (ITOEC)*, Chongqing, China, Oct. 2017, pp. 69–72.
- [3] M. Perkovič, L. Gucma, M. Bilewski, B. Muczynski, F. Dimc, B. Luin, P. Vidmar, V. Lorenčić, and M. Batista, "Laser-based aid systems for berthing and docking," *J. Mar. Sci. Eng.*, vol. 8, no. 5, pp. 1–21, 2020.
- [4] T. Wang, "Research on ship berthing monitoring technology based on 3D laser point cloud data," in *Proc. IEEE Int. Conf. Saf. Produce Inf. (IICSPI)*, Dec. 2018, pp. 165–168.
- [5] K. Maritime. *Relative Position Reference System RADIUS*. Accessed: Dec. 17, 2020. [Online]. Available: <https://www.kongsberg.com/maritime/products/vessel-reference-systems/position-systems/relative-position-reference-system-radius/>.
- [6] Y. Mizuchi, Y. Choi, Y. Kim, Y. Hagiwara, and T. Ogura, "Vision-based markerless measurement system for relative vessel positioning," *IET Sci., Meas. Technol.*, vol. 10, no. 6, pp. 653–658, Sep. 2016.
- [7] H. P. Yuen, Y. W. Choi, and Y. B. Kim, "Implementation of Tracking-Learning-Detection for improving of a Stereo-Camera-based marker-less distance measurement system for vessel berthing," in *Proc. 16th IEEE Int. Colloq. Signal Process. Its Appl. (CSPA)*, Langkawi, Malaysia, Feb. 2020, pp. 63–68.
- [8] H. Kim, J. Koo, D. Kim, B. Park, Y. Jo, H. Myung, and D. Lee, "Vision-based real-time obstacle segmentation algorithm for autonomous surface vehicle," *IEEE Access*, vol. 7, pp. 179420–179428, 2019.
- [9] NVIDIA. *Technical Specifications of Jetson TX2 Module*. Accessed: Dec. 17, 2020. [Online]. Available: <https://developer.nvidia.com/embedded/jetson-tx2>
- [10] B. Cai, X. Xu, K. Jia, C. Qing, and D. Tao, "DehazeNet: An End-to-End system for single image haze removal," *IEEE Trans. Image Process.*, vol. 25, no. 11, pp. 5187–5198, Nov. 2016.
- [11] R. Fattal, "Dehazing using color-lines," *ACM Trans. Graph.*, vol. 34, no. 1, pp. 1–14, Dec. 2014.
- [12] D. Makkar, D. of RIMT Chindana India, and M. Malhotra, "Single image haze removal using dark channel prior," *Int. J. Eng. Comput. Sci.*, vol. 4, pp. 2341–2352, Jan. 2016.
- [13] W. K. Pratt, *Digital Image Processing*, 4th ed. Hoboken, NJ, USA: Wiley, 2007.
- [14] K. H. Lim, C. H. Lim, W. L. Lim, and H. E. Yap, "Differential settlement monitoring system using inverse perspective mapping," *IEEE Sensors J.*, vol. 18, no. 6, pp. 2545–2554, Mar. 2018.
- [15] W. Yang, B. Fang, and Y. Y. Tang, "Fast and accurate vanishing point detection and its application in inverse perspective mapping of structured road," *IEEE Trans. Syst., Man, Cybern. Syst.*, vol. 48, no. 5, pp. 755–766, May 2018.
- [16] U. Ozgunalp, "Robust lane-detection algorithm based on improved symmetrical local threshold for feature extraction and inverse perspective mapping," *IET Image Process.*, vol. 13, no. 6, pp. 975–982, May 2019.
- [17] M. Oliveira, V. Santos, and A. D. Sappa, "Multimodal inverse perspective mapping," *Inf. Fusion*, vol. 24, pp. 108–121, Jul. 2015.



**HANGUEN KIM** (Member, IEEE) received the B.S. and M.S. degrees from Kyunghee University, Suwon, South Korea, in 2009 and 2011, respectively, and the Ph.D. degree from the Korea Advanced Institute of Science and Technology (KAIST), Daejeon, South Korea, in 2016.

From 2015 to March 2017, he worked as a Managing Researcher with Samsung S1 Corporation. He is currently the Director of Seadronix Corporation, Daejeon. His research interests include deep learning (deep neural networks), computer vision, human–computer interaction, and robot navigation.



**DONGHOON KIM** (Member, IEEE) received the B.S. degree from the University of Seoul, Seoul, South Korea, in 2009, and the M.S. and Ph.D. degrees from the Korea Advanced Institute of Science and Technology (KAIST), Daejeon, South Korea, in 2011 and 2016, respectively.

He is currently the Director of Seadronix Corporation, Daejeon. His research interests include deep learning (deep neural networks), computer vision, surface robots, and robot navigation.



**BYEOLTEO PARK** (Member, IEEE) received the dual B.S. degrees in electrical engineering and civil engineering and the M.S. and Ph.D. degrees in civil engineering from the Korea Advanced Institute of Science and Technology (KAIST), Daejeon, South Korea, in 2010, 2011, and 2016, respectively.

He is currently the CEO of Seadronix Corporation, Daejeon. His research interests include the areas of SLAM (simultaneous localization and mapping), robot navigation, underground localization, indoor localization, artificial intelligence, and unmanned surface vehicle.



**SEUNG-MOK LEE** (Member, IEEE) received the Ph.D. degree in civil and environmental engineering (robotics program) from the Korea Advanced Institute of Science and Technology (KAIST), Daejeon, South Korea, in 2014.

From 2014 to 2015, he was a Postdoctoral Fellow with the Urban Robotics Laboratory, KAIST. From 2015 to 2017, he was a Senior Research Engineer with the Intelligent Safety Technology Center, Hyundai Motor Company, Hwaseong, South Korea. Since 2017, he has been an Assistant Professor with the Department of Automotive System Engineering, Keimyung University, Daegu, South Korea. His current research interests include soft computing, autonomous vehicles, simultaneous localization and mapping, and robot navigation.

...